An optical counterjet in 3C66B?

Didier Fraix-Burnet

Mon. Not. R. Astron. Soc. **226**, 1–7 (1996) Printed 27 July 2004 (MN plain TEX macros v1.6)

An optical counterjet in 3C66B?

D. Fraix-Burnet

Laboratoire d'Astrophysique UMR 5571, Observatoire de Grenoble, BP 53, F-38041 Grenoble Cédex 9, France, fraix@gag.observ-gr.fr

Accepted September 1996 . Received July 1996 ; in original form 1996 July 1

ABSTRACT

Long exposure observations at the Canada-France-Hawaii Telescope of 3C66B in the I filter are presented. After subtraction of the galactic background, optical emission on the counterjet side is detected in 10 knots coincident with the radio counterjet. Their radio-to-optical spectral indices (0.5–0.6) are typical of synchrotron emission in extragalactic jets, so that these knots possibly are the optical counterparts of the radio counterjet. If this is confirmed, 3C66B would be the first double-sided extragalactic optical jet. The optical counterjet would also be brighter than what is predicted from the relativistic beaming interpretation of brightness asymmetry between the two jets. This would thus prove that the radiation properties are intrinsically different in the two jets. Alternatively, these knots could have nothing to do with the counterjet. But it seems that in this case, the optical counterjet would be fainter than expected from the relativistic beaming interpretation, favouring intrinsic asymmetry as well. In addition, two new optical components are found in the jet.

Key words: methods: observational – galaxies: individual: 3C66B – galaxies: jets

1 INTRODUCTION

The spectrum of extragalactic jets is a pure synchrotron continuum, which is essentially a power-law. This characteristic does not facilitate the determination of the material velocity within the jet. Motions detected at the parsec-scale close to the nucleus and also now at kpc-scales in M87 (Biretta, Zhou & Owen 1995) are the only means of measuring velocities. This gives however only the speed of radiating particles, not that of the bulk of the jet. The two have to be distinguished because they represent two different physics (Sol, Pelletier & Asséo 1989; Pelletier & Roland 1986, 1988; Fraix-Burnet & Pelletier 1991; Fraix-Burnet 1992; Despringre & Fraix-Burnet 1996).

Brightness asymmetries between jets and their counterjets in radiosources are generally believed to be apparent and due to Doppler effects. But obviously, there are intrinsic structural differences in a lot of double-sided jets, so that this relativistic interpretation can be questioned. From theoretical and observational evidences, Fraix-Burnet (1992) argued that the jet asymmetries in radiosources are mainly due to intrinsic differences in radiation properties. To distinguish between these two interpretations, one should compare the physics of the jet and counterjet. This is however very difficult with a power-law continuum spectrum. The spectral index is Lorentz invariant, so that it should be the same in the two jets. A check of this point would require observations at three frequencies, including millimetre or even submillimetre data, i.e. away enough from the break frequency which is not Lorentz invariant.

The cutoff frequency of the synchrotron spectrum is a second characteristic which is very sensitive to local physical conditions within the jet. It is unknown for nearly all extragalactic jets (being in the sub-mm or far-infrared domain) except for the very few cases where the synchrotron radiation is seen in the optical: M87, 3C273, 3C66B, PKS0521-36, 3C264 (Crane et al. 1993), and 3C78 (Sparks et al. 1995). The precise shape of the cutoff is known for only the three brightest: M87 (Biretta, Stern & Harris 1991; Meisenheimer, Röser & Schlötelburg 1996), 3C273 (Fraix-Burnet & Nieto 1988) and 3C66B (Fraix-Burnet, Golombek & Macchetto 1991). All known optical jets are one-sided both in the optical and in the radio, with the notable exception of 3C66B which shows a counterjet in the radio (Leahy, Jägers & Pooley 1986; Hardcastle et al. 1996). If the relativistic interpretation for asymmetry is correct, the counterjet should also radiate in the optical and should have the same intrinsic spectrum. By deriving the Doppler factor from the jet to counterjet intensity ratio in the radio, it is then possible to compute the Doppler shifted spectrum of the counterjet from the observed spectrum of the jet. 3C66B is the only source for which this is feasible. At a distance of 86 Mpc (for $H_0 = 75$ km s^{-1} Mpc^{-1}), 1 arcsec is equivalent to 417 pc in this object.

The present study aims at detecting the optical counterjet in order to discriminate between the two interpretations for brightness asymmetry and to help in understanding why so few jets are seen at optical wavelengths. After a presentation of the observations (Sect. 2) and a description of the results (Sect. 3), a discussion on whether the detected structures belong to the jet will be made in Sect. 4, together with a comparison of the present results with the prediction of the

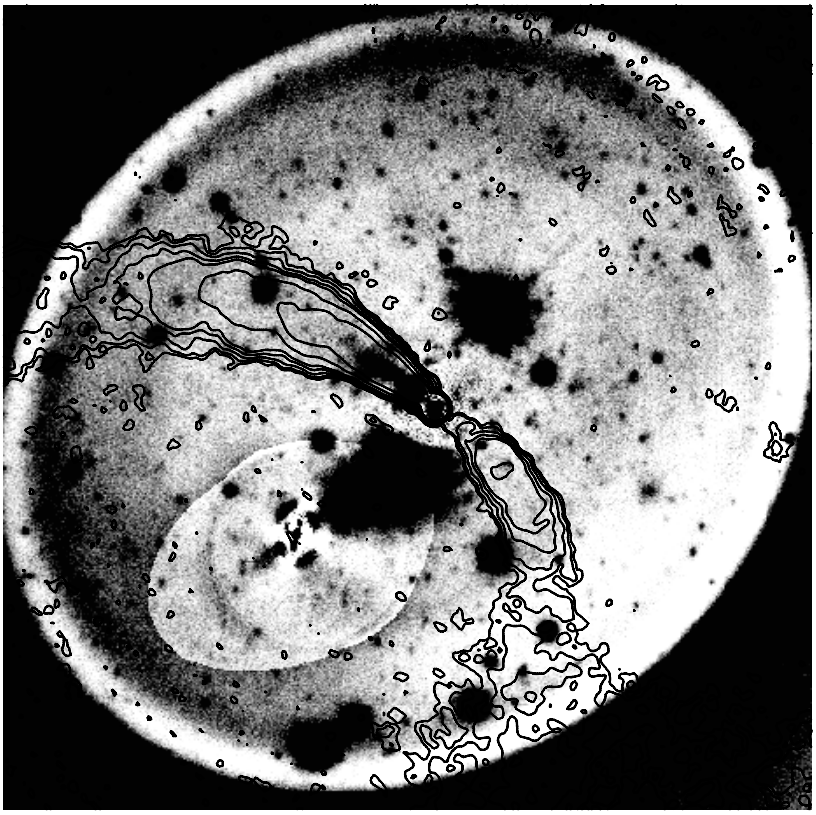

Figure 1. Residues after subtraction of elliptical models of 3C66B and its companion. The square field is 100 arcsec wide, and cuts are -0.9 (white) to 2.5 (black) μJy/arcsec^2. Overlaid are contours of the 8 GHz 1.25 arcsec resolution map from Hardcastle et al. (1996).

relativistic interpretation.

2 OBSERVATIONS AND DATA REDUCTION

Observations were made at the Canada-France-Hawaii Telescope (CFHT) on September 24-27 and November 23-29, 1995. The detector was MOCAM, but only one of the four 2048×2048 CCDs (chip U2) was used. The scale of 0.204 arcsec per pixel provides a 7 arcmin field of view. The galaxy 3C66B was placed near the upper (North) border of the chip so that the very bright star 1.3 arcmin to the North was out of the CCD avoiding saturation spikes over the galaxy. To avoid non-linearity at high exposure levels on the center of 3C66B (for galactic background modelling and photometric purposes), the exposure time was limited to 10 minutes, except for 3 exposures taken through clouds where the integration time was set to 20 minutes. 85 images through the I filter were obtained totalling nearly 15 hours of exposure time. The FWHM of the images varied from 0.75 to 1.6 arcsec with a strong concentration between 0.8 and 1.2 arcsec. The data were divided in two equal groups above and below FWHM= 1 arcsec (respectively 43 and 42 images). The medians of the high-resolution and low-resolution groups have FWHM of 0.90 and 1.14 arcsec respectively, while the total median of all images have FWHM= 1.01 arcsec.

Elliptical modelling of the galaxy 3C66B and its companion (at 23 arcsec to the SE) were performed with the ISOPHOTE package within IRAF. This task is complicated by a 13.7 I-magnitude star at 14 arcsec to the NNW of 3C66B. The result of the subtraction of this elliptical model (up to a radius of 40 arcsec) is shown in Fig. 1. The modelling has been optimized so that the background around the jet and counterjet is as flat as possible. As can be readily seen in Fig. 1 and Fig. 2, there are 3 regions where the residues reveal an excess over this elliptical isophotal shape of the galaxy (the dark patch 14 arcsec to the NNW is the 13.7 I-magnitude star). There is a big region between the centers of 3C66B and its companion. This might be the clear signature of the interaction between both galaxies. Two arc-like regions are visible on the jet at about 4 and 9 arcsec from the nucleus. These three regions could be removed in the elliptical fitting process, but with the appearance of strong negative regions. I thus consider that they are real regions of the galaxy that depart from elliptical modelling of 3C66B. No further attempt to remove them was done because they do not intervene in the counterjet region, the main goal of this work. The companion removal has not been optimized also as can be seen on Fig. 1 and has been done essentially to ease the elliptical fitting of 3C66B and to get a flat background around the jet and counterjet. This background is however very slightly negative in some places.

Flux calibration of the data used the photoelectric aperture photometry by Keel (1988): $M_I = 13.18 \pm 0.02$ within a 21 arcsec radius. The same measurement was performed on the total, high- and low-resolution median images to obtain the calibration constant. The noise level was then estimated to be 0.02 μJy per pixel on the total median image that will be considered in the following.

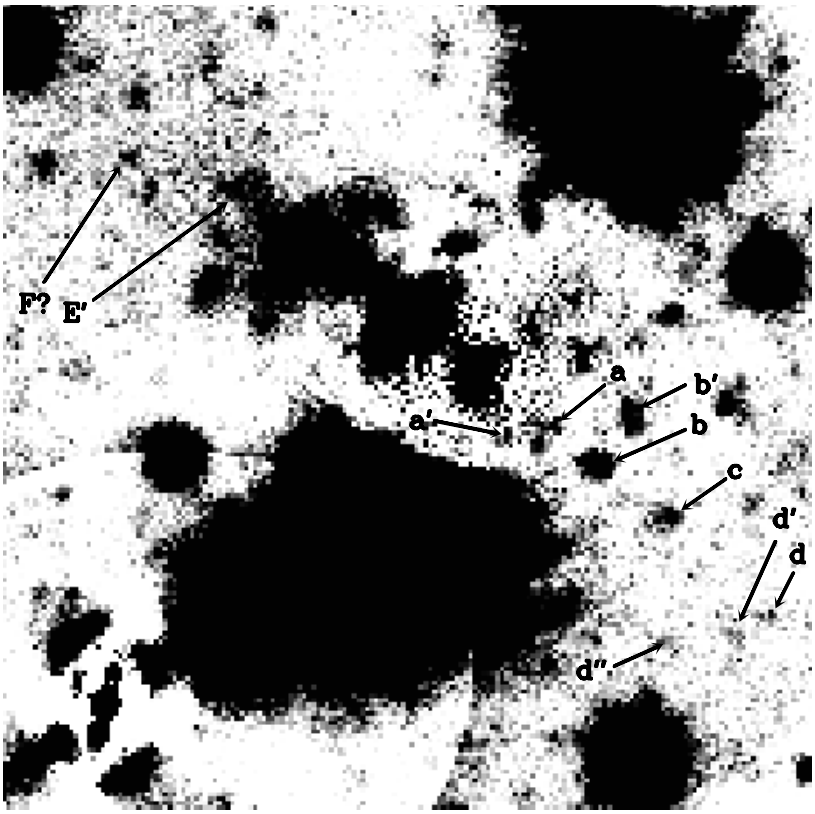

Figure 2. Center 37 arcsec square field of Fig. 1 showing new features that can be related to the jet and counterjet (white: 0 and black: 1.5 μJy/arcsec^2).

Table 1 Knots characteristics: d is the distance from the center of 3C66B in arcsec, PA is the position angle in degrees, I is the total intensity (μJy) integrated over a circular area of radius r (arcsec), and the radio intensity (μJy) is measured from the 1.25 arcsec resolution 8 GHz map by Hardcastle et al. (1996) within the same area. The spectral index is computed from the radio and I intensities.

Knots	d	PA	I	r	Radio intensity	Spectral index
Counterjet:						
a	4.5	47 + 180	1.4	0.8	244	0.48
a'	3.6	23 + 180	0.3	0.4	–	–
b	7.3	52 + 180	3.6	0.8	659	0.48
b'	7.1	73 + 180	2.3	0.8	95	0.35
c	11.3	53 + 180	1.2	0.6	642	0.58
d	17.7	50 + 180	0.3	0.4	150	0.59
d'	17.1	44 + 180	0.2	0.4	167	0.61
d"	15.3	34 + 180	0.3	0.4	151	0.59
Jet:						
A	1.3	51	1.6	0.4	4768	0.75
B	2.9	51	18.8	0.6	11461	0.60
C	4.1	53	16.2	0.6	8892	0.59
D	5.8	51	6.5	0.6	5518	0.63
E	7.4	53	7.2	0.6	5409	0.62
E'	13.2	52	1.5	0.6	2464	0.69
F	18.3	59	0.5	0.4	916	0.71

3 RESULTS

The median of the 85 images is shown on Fig. 1. The outermost isophotes are uncertain because of the proximity of the edge of the CCD to the North. The jet is clearly visible and overlaid contours of the radio galaxy (Hardcastle et al. 1996) illustrate the relative sizes of the optical jet and the two radio jets. A lot of small patches are seen which could be foreground stars, but also globular clusters or background galaxies because of their somewhat extended shape.

3.1 On the counterjet side

A closeup view of the optical jet and counterjet regions is presented in Fig. 2 and 3. Labelling of new potentially interesting components is given in Fig. 2. Their interest is largely justified in Fig. 3 where the radio contours are overlaid. Knots a, b, c, d, d' and d" are spatially coincident with radio features, while knots b' could well be related to the jet. Knot a' will not be considered further on in this paper since it has no radio counterpart even though it is extremely close to the radio jet. Of course, numerous foreground stars are present throughout the field of the CCD and a few 'knots' can be seen just North of the counterjet. It is difficult to distinguish the labelled knots with the others, and except maybe for knot c, they do not seem to be stellar. There is no clear excess of such 'knots' in the region of the counterjet as compared with the 7 arcmin field of the entire CCD, as can also be seen from Fig. 1. Thus, one cannot rule out chance coincidence of totally unrelated objects.

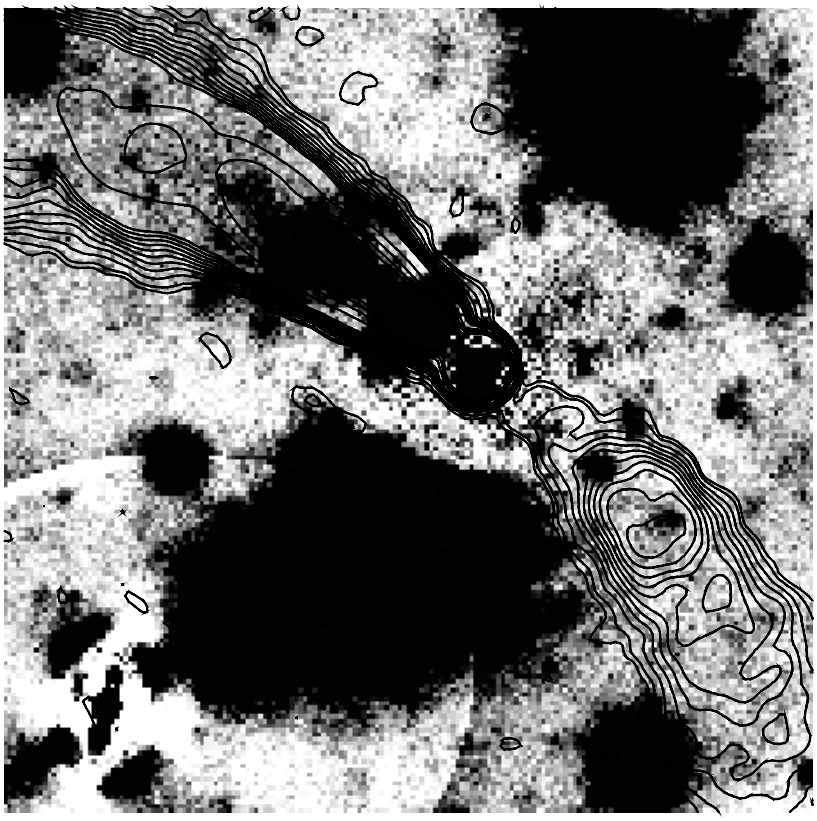

Figure 3. Same as Fig. 2 (white: -0.9 and black: 1.5 μJy/arcsec^2) with radio contours added (levels: 0.05, 0.1, 0.2,...,, 1, 2,..., 5 mJy/beam).

Positions and intensities of these knots are given in Table 1. The spectral indices are similar for all these knots (except b') and are slightly lower than those found in the jet. Note that the same spectral indices (within 0.02) are found with the 0.75 arcsec resolution map by Hardcastle et al. (1996).

3.2 The jet

Two features newly seen in the optical are labelled on Fig. 2 and described in Table 1. Knot E' is a new optical component of the jet, as can be clearly seen on Fig. 4. Knot F has been identified from the radio by Hardcastle et al. (1996) and there is an optical component which is here tentatively identified with it. However, as in the case of the counterjet, it is impossible from the present study to assert that this component is really the optical counterpart of radio knot F.

The similarity of contours in the radio and optical is obvious on Fig. 4. This is confirmed by the spectral index (Table 1) being essentially constant (excepting knot A) up to about 8 arcsec from the nucleus (Jackson et al. 1993). Knots E' and F have a slightly higher spectral index.

4 DISCUSSION

With observations in only one filter, it is difficult to determine whether the identified knots belong to the counterjet. They do not appear stellar, except may be for knot c. Comparison between elliptical gaussian fits of these knots made on the high-resolution and the low-resolution median images do not point to a stellar nature. The spectral indices (between 0.5 and 0.6) derived by assuming they belong to the counterjet (Table 1) are consistent with synchrotron radiation generally found in jets. Only knot b' departs from this figure. It is thus entirely plausible that at least a few of these knots are the optical counterparts of the radio jet.

Let us compare our results with the prediction of the relativistic interpretation of brightness asymmetry between the jet and the counterjet. In this interpretation, the difference in brightness is explained solely by the Doppler effect. For a spectrum with a constant spectral index α, one has: $I_j/I_{cj} = (D_j/D_{cj})^\delta = \mathrm{D}^\delta$ where I_j (I_{cj}) is the jet (counterjet) intensity at a given observational frequency, D_j (D_{cj}) is the jet (counterjet) Doppler factor, and $\delta = 3+\alpha$ ($\delta = 2+\alpha$ for a filled and uniform jet; Blandford and Königl, 1979). By assumption in the relativistic interpretation, the physics of the jet and the counterjet is the same, so that α is identical for both. The intensity ratio between the two jets in the radio yields $\mathrm{D} = D_j/D_{cj} = (1+\beta\cos\theta)/(1-\beta\cos\theta)$ which is characteristic of the jet and does not depend on the frequency of the observations. Following Hardcastle et al. (1996), $\alpha = 0.5$ between 8 and 15 GHz and D is about 2.2 below 7 arcsec from the nucleus and about 1.5 between 7 and 19 arcsec with $\delta = 3+\alpha$ (respectively 3.1 and 1.7 with $\delta = 2+\alpha$). The counterjet intensity measured in the I filter then corresponds roughly to the intensity of the jet as measured in the U filter (Fig. 5). Since the cutoff frequency is in this region of the spectrum, α varies and the expected intensity ratio between the counterjet and the jet is much lower than the same ratio in the radio (Fig. 5). We thus have: $I_{cj}(I) \simeq I_j(U)\ (D_j/D_{cj})^{-3}$ or $\simeq I_j(U)\ (D_j/D_{cj})^{-2}$ depending on the choice for δ. Taking the intensity $I_j(U) \simeq 1.1$ μJy of the brightest knot B from Fraix-Burnet et al. (1989):

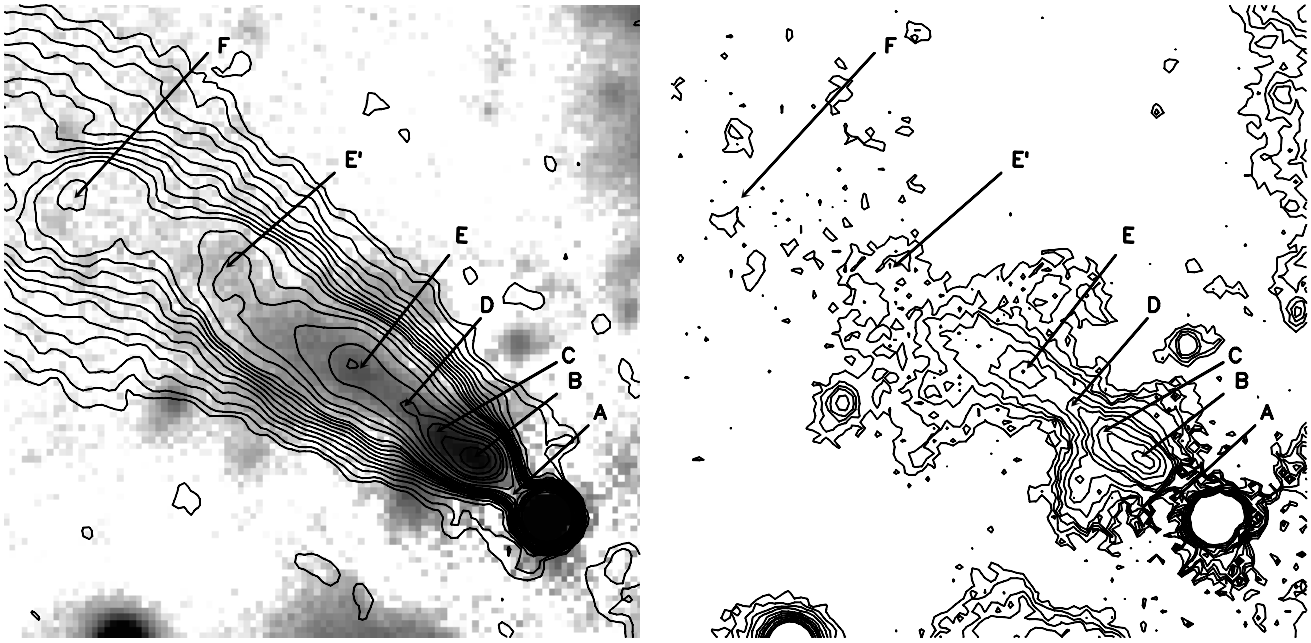

Figure 4. *Left:* Image of the jet overlaid by radio contours of the 0.75 arcsec resolution map by Hardcastle et al. (1996) (levels: 0.05, 0.1, 0.2,..., 1.0, 1.25, 1.5, 2, 3, 4, 5, 7, 10 mJy/beam). The square field is 20 arcsec wide. Knots A, B, C, D, E have been labelled by Fraix-Burnet et al. (1989) and F is a radio knot defined by Hardcastle et al. (1996). Knot E' is a new optical knot found in this paper that corresponds to a very distinct radio feature. *Right:* Optical contours (levels: 0.03, 0.06, 0.09, 0.13, 0.19, 0.25, 0.32, 0.38, 0.51, 0.63, 0.76 μJy/arcsec^2) with the same labelling as previously. Note the similarity between the optical contours and the radio ones on the figure to the left.

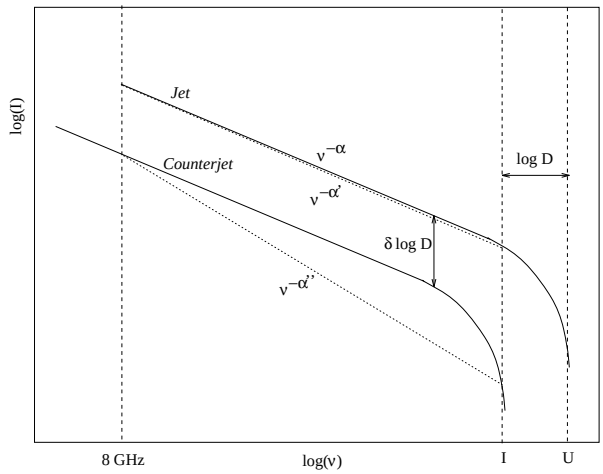

Figure 5. The effect on the synchrotron spectrum (of spectral index α) of a Doppler shift between the jet and the counterjet. The dotted line gives the observed radio-to-optical spectral index ($\alpha' > \alpha$) of the jet, and the expected one ($\alpha'' > \alpha'$) for the counterjet following the relativistic interpretation. Symbols 'I' and 'U' stand for the corresponding filters. $\delta = 3 + \alpha$ or $2 + \alpha$ depending on the jet model. D is the relative Doppler factor.

$I_{cj}(I) \simeq 0.1$ μJy below 7 arcsec and $\simeq 0.35$ μJy farther away. This is well above the noise level of the total median image (see Sect. 2). Hence the present data should reveal the equivalent of knot B for the counterjet, if it is the perfect symmetric of the jet.

Strictly speaking, there is no symmetric knot to knot B, so that the optical emission of the counterjet is fainter than what is predicted by the relativistic interpretation. But, if the detected knots belong to the counterjet, all the 'inner' ones ($d < 7$ arcsec) are much brighter than the expected 0.1 μJy. The 'outer' knots of the jet (E and F) have U intensities 2 to 3 times lower than knot B, so that the expectation in the symmetric region on the counterjet side is rather $\simeq 0.13$ than 0.35 μJy as stated above. All corresponding knots are significantly brighter than this. As a conclusion, all identified knots for the counterjet are brighter than the predicted value from the relativistic interpretation. They even have smaller radio-to-optical spectral indices (see Table 1) than the jet, in total contradiction with the relativistic interpretation (Fig. 5) which predicts larger spectral indices. The values for the spectral index (about 0.5-0.6) are fully consistent with a synchrotron origin for the optical emission and correspond to values generally found in jets. The only exception is knot b' which has a very low spectral index (0.35) so that its link with the radio jet can be questioned.

The consequence is that the detected knots, if belonging to the counterjet, prove that the radiation properties are intrinsically different in the jet and in the counterjet. The counterjet is less bright in the radio implying fewer radiating particles as a whole or a lower magnetic field. Since the radio-to-optical spectral index is smaller, the cutoff frequency in the counterjet is higher, which is consistent with a lower magnetic field.

5 CONCLUSION

The search for the first optical extragalactic counterjet has yielded several components that are coincident with the radio counterjet. However, it is not possible to determine precisely the origin of the optical emission. Still deeper images or observations in another filter are needed. From the radio-to-optical spectral index of these components, it is quite plausible that they are the optical counterparts of the radio counterjet. If this is the case, smaller spectral indices are found than for the jet, in contradiction with the prediction by the relativistic beaming interpretation of brightness asymmetry between the jet and the counterjet. This indeed means that the physics of the counterjet is intrinsically different from that of the jet: the magnetic field seems to be weaker in the counterjet, so that the radio intensity is lower and the cutoff frequency higher. Alternatively, if the detected knots have no relation with the counterjet, then our data seem to indicate that its optical emission is fainter than what is predicted by the relativistic beaming interpretation, favouring again an intrinsic brightness asymmetry.

ACKNOWLEDGMENTS

These observations have been obtained while being visitor astronomer at the Canada-France-Hawaii Telescope, operated by the Conseil National de la Recherche of Canada, the Conseil National de la Recherche Scientifique of France and the University of Hawaii. I thank M. Crézé, J.-C. Cuillandre, Y. Mellier and A. Robin, for obtaining some of the data. M.J. Hardcastle very kindly provided the electronic radio images.

REFERENCES

Biretta J.A., Stern C.P., Harris D.E., 1991, AJ 101, 1632
Biretta J.A., Zhou F., Owen F.N., 1995, ApJ 447, 582
Blandford R.D., Königl A., 1979, ApJ 232, 34
Crane et al., 1993, ApJ 402, L37
Despringre V., Fraix-Burnet D., 1996, A&A submitted
Fraix-Burnet D., 1992, A&A 259, 445
Fraix-Burnet D., Golombek D., Macchetto F.D., 1991, AJ 102, 562
Fraix-Burnet D., Nieto J.-L., 1988, A&A 198, 87
Fraix-Burnet D., Nieto J.-L., Lelièvre G., Macchetto F.D., Perryman M.A.C., di Serego Alighieri S., 1989, ApJ 336, 121
Fraix-Burnet D., Pelletier G., 1991, ApJ 367, 86
Hardcastle M.J., Alexander P., Pooley G.G., Riley J.M., 1996, MNRAS 278, 273
Jackson N., Sparks W.B., Miley G.K., Macchetto F., 1993, A&A 269, 128
Keel W.C., 1988, ApJ 329, 532
Leahy J.P., Jägers W.J., Pooley G.G., 1986, A& A 156, 234
Meisenheimer K., Röser H.-J., Schlötelburg M., 1996, A&A 307, 61
Pelletier G., Roland J., 1986, A&A 163, 9
Pelletier G., Roland J., 1988, A&A 196, 71
Sol H., Pelletier G., Asséo E., 1989, MNRAS 237, 411
Sparks W.B., Golombek D., Baum S.A., Biretta J., de Koff S., Macchetto F., McCarthy P., Miley G.K., 1995, ApJ 450, L55

This paper has been produced using the Royal Astronomical Society/Blackwell Science TEX macros.